3D Localization of Neurons in Bright-Field Histological Images

Andrija Štajduhar[1, 2, 3], Claude Lepage[3], Miloš Judaš[1], Sven Lončarić[2], Alan C. Evans[3]
[1] Croatian Institute for Brain Research, School of Medicine, University of Zagreb, Šalata 3, Zagreb, Croatia
[2] Faculty of Electrical Engineering and Computing, University of Zagreb, Unska 3, Zagreb, Croatia
[3] Montreal Neurological Institute, McGill University, 3801 University Street, Montreal, Quebec, Canada
astajd@astajd.com

***Abstract*—In this paper, we present a method for inferring the depth of neurons found in a bright-field microscopic image of a histological section of a human brain, digitized at high resolution in multiple planes along the z-axis. Individual neuron bodies are segmented and tracked throughout the depth of the whole image stack and placed at the appropriate z-level in the stack based on variations in image sharpness.**

***Keywords*—High-resolution Imaging; Digital Microscopy; Immunohistochemistry**

I. Introduction

Technological advances in the past several decades have empowered scientists in life sciences to analyze data in hitherto unseen detail. Whole slide digital imaging enables (i) the digitization of histological preparations of various types, and (ii) provides the capacity to store, share and analyze tissue specimens with the same level of detail as one would observe under the lens of a microscope [1]. However, as is most often the case, objects whose nature is three-dimensional are captured by a camera that produces a series of two-dimensional images.

The 3D context provides a more detailed and realistic insight in cellular organization and is therefore more anatomically meaningful. This is especially relevant for studies in which several consecutive sections are registered to produce a 3D volume. For instance, if the sections are cut with a 20μm thickness but scanned at 1μm in-plane resolution, we benefit from the higher scanning resolution only in the horizontal plane, while the 3D resolution remains limited by the section thickness. By accurately positioning the cells within the section in 3D, one can better approach an isotropic 3D resolution and obtain realistic and continuous distribution of cells across the volume. Such analysis may more accurately reveal subtle changes in cellular organization, columnar formation and underlying tissue cytoarchitectonics.

In this paper, we examine the use of multi-level scanning of bright-field images of histological preparations along the z-axis. We propose an automatic determination of neuron locations in three dimensions by combining the in-plane neuronal depth information from adjacent 2D planes into full 3D neuronal localization.

A. Neuron imaging in 3D

To visualize cells in the tissue and examine its cellular layout, a histological preparation is made. The tissue of interest is cut into thin sections and treated with various stains to enhance inherently small visual contrast in such sections and highlight features of interest. The stained tissue is then mounted on a glass slide and ready for examination under the microscope, to be digitized using a histological scanner, or to be stored for future examination.

Most of today's histological slides are examined using bright-field (non-confocal) imaging, because of the compatibility with the histological staining methods used in slide preparation. In these methods, a histological slide being examined is homogeneously illuminated with the background light and captured through the lens of a microscope. Stained neurons absorb the light and are shown as areas of dark contrast on a brighter background. This microscopy modality is also referred to as transillumination or transmitted light microscopy [2], or sometimes as wide-field microscopy because of the whole slide being illuminated (Fig. 1). The limitation of this modality for 3D analysis of cellular locations is the presence of background signal from out-of-focus structures throughout the slide. To determine an accurate 3D depth of a neuron in the tissue, a researcher relies on subtle adjustments in focusing using finely-tuned focusing wheels while observing the individual neurons under the lens of a microscope, which is very slow and time consuming.

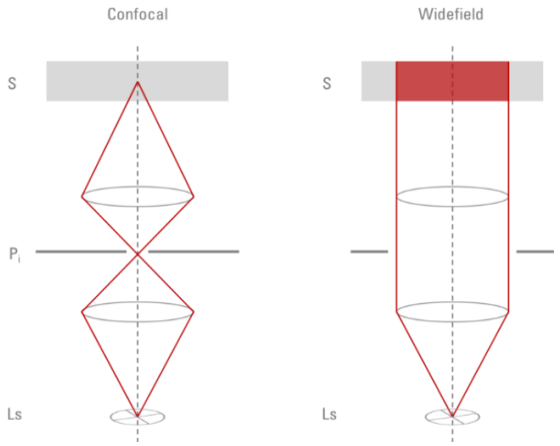

Figure 1: Confocal and wide-field illumination. In confocal imaging, light from the source (Ls) is focused through a pinhole (Pi) and subsequently into the sample (S) resulting in a relatively small volume being observed. In wide-field imaging, histological slide being examined is homogeneously illuminated with the background light. Image reproduced from [3].

In confocal imaging, a tissue section is stained using fluorescent dyes that emit light under excitation by laser units located within the confocal microscope. The emitted light is captured using a light-sensitive camera and the image is formed. Using precisely focused laser beams, which are spatially filtered through a pinhole aperture, it is possible to obtain a signal from a single focal plane, hence the name 'confocal'. By creating z-series through the depth of the tissue it is possible to reconstruct cells in the tissue. Confocal imaging produces tomography-style cellular imaging data that provide richer information about 3D neuronal structures, with less noise from background and out-of-focus structures. There are successful methods for cell tracking and reconstruction that consider the context of neuron imaging in 3D using confocal or other similar imaging modalities [4-7]. However, due to the nature of fluorescent dyes, confocal preparations suffer from photobleaching and photodamage and are viable only for a limited amount of time. Also, they are not appropriate for whole slide imaging as the image capturing field is very narrow, but are rather used in detailed analysis of smaller structures like dendritic spines and axonal arborization.

Vast collections of histological sections that were stained in traditional methods are not suitable for inspection under confocal microscopes. Histological slides produced in large scale histological database, such as the BigBrain [8], are usually produced using a bright-field imaging modality. However, we can leverage the use of multilevel image acquisition, produce images of histological sections at multiple optical levels and derive spatial data based on changing sharpness of objects that are tracked along the z-axis of the section stack. This procedure resembles the above-mentioned traditional manual approach used by anatomists to track neurons along the z-axis by adjusting the microscope's focus.

II. Materials and Methods

Our aim was to develop a procedure that, based on given locations of neurons in 2D, adds another coordinate to each neuron location, placing it within the 3D space of the histological slide. This section details the procedures we performed as well as the nature of the images used.

A. Dataset

We used histological sections of an adult human brain that were stained using NeuN, a common immunohistochemistry method that is used for labelling neurons in the brain tissue. Samples were obtained from the Zagreb Brain Collection [9] and scanned using the Hamamatsu Nanozoomer 2.0 scanner (Hamamatsu Photonics, Japan), using multiple optical planes. An example of a neuron at different focal planes is shown on Fig. 2. Images were acquired from a section of 10µm thickness using 11 optical planes with 1µm step at 40x magnification, which corresponds to 0.226µm/pixel resolution. The NDPI files produced by the scanner were several gigabytes in size, making the whole slide processing infeasible. Therefore, we extracted smaller image patches using open source software NDPITools [10] for each optical plane, created image stacks and processed them separately. Initial locations of individual cells in (x, y)-plane were found in the image at mid-plane using the automatic approach for neuron detection in NeuN-stained sections described in [11].

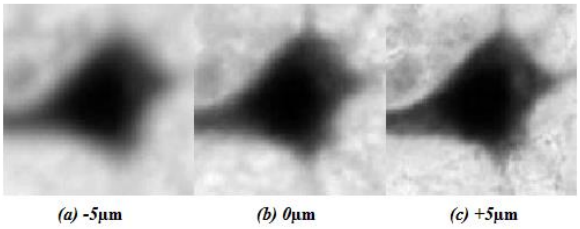

Figure 2: A neuron body at different focal planes. Shown here are planes at (a) -5µm, (b) 0µm and (c) +5µm offset. This neuron was found to have greatest measure of sharpness in the plane (c).

B. Segmentation of neuron bodies

For delineating neuron borders and separating closely located neurons in the tissue, we used a watershed algorithm to create basins each containing a single neuron. Since the nature of the staining used is such that it amplifies the contrast between the neurons and the rest of the tissue, neurons are clearly visible with distinguishably brighter background. We used Otsu's method [12] to separate neuron bodies from the background in each watershed basin and obtain image pixels that belong to individual neurons. Pixels within the borders of the neurons were used for measuring the neuron sharpness at each z-level. Watershed basins as well as outlines of neurons are shown on Fig. 3.

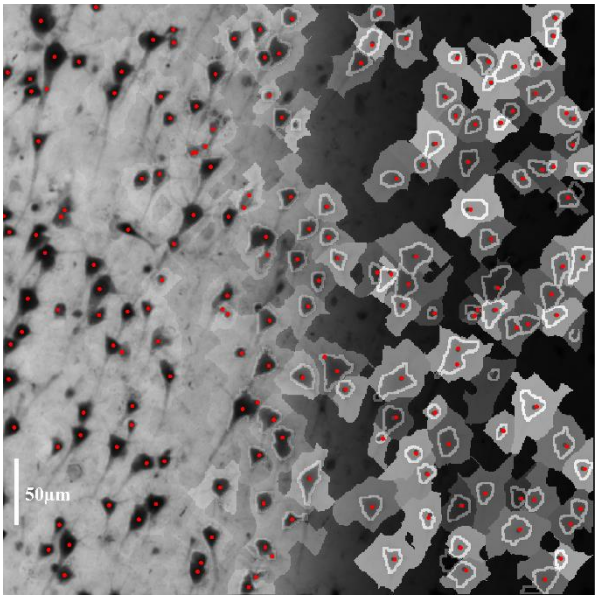

Figure 3: Image showing an example of digitized histological slide using bright-field imaging, locations of neurons and watershed basins with outlined neuron borders. Pixels within the borders are used for measuring the neuron sharpness at each z-level.

C. Image sharpness

To determine the central location of each neuron along the z-axis, we relied on the sharpness of the neuron body across all images in the stack to determine the level at which the maximum sharpness was obtained. After reviewing a comparison of several focusing measures [13], we used the Variance of

Laplacian metric, applied to the intensity of those pixels belonging to a neuron body, as the measure of neuron sharpness. For a neuron n, at z-level l, we compute the focusing measure using the formula

$$\phi_{n,l} = \sum_{(x,y)\in\Omega_{n,l}} (\Delta I(x,y) - \overline{\Delta I})^2, \quad (1)$$

where $\Omega_{n,l}$ is (x, y)-domain of the neuron and $\overline{\Delta I}$ is the mean value of the image Laplacian within $\Omega_{n,l}$. This measure was first proposed in [14] for the use of autofocusing in microscopy. It is inexpensive to compute, insensitive to image noise and produces scalar outputs that can be easily compared across the section stack. To obtain the Laplacian of the images, we convolved each image in the stack with the discrete Laplacian operator

$$L = \begin{bmatrix} 0 & 1 & 0 \\ 1 & -4 & 1 \\ 0 & 1 & 0 \end{bmatrix} \quad (2)$$

The rationale for choosing this measure is as follows. If a neuron in a level along z-axis is out of focus, its pixels, and especially pixels along the border of the neuron, will be blurred, resulting in low variation of the signal, less sharper edges and lower gradient magnitude. This will also be reflected on the Laplacian which will have less dispersed values in blurred image areas. The opposite will happen in the image at the correct z-axis for a neuron of interest. Therefore, to correctly place each neuron in the observed tissue patch, we identify the z-level that has the maximum $\phi_{n,l}$ variance of Laplacian of the pixels in the neuron body.

D. Spline interpolation

After obtaining the third spatial dimension from 2D data as described above, the resulting z-coordinates will still fall under the number of focal layers in which the slide was scanned. To make neuron locations more realistic in 3D, we interpolated the measurements of neuron sharpness across the section stack and, instead of choosing the layer in which the sharpness measure is largest, we used z-value where the maximum of the spline is achieved (Fig. 4). This allows for neurons to be located with continuous z-coordinate instead of having limited set of possible values.

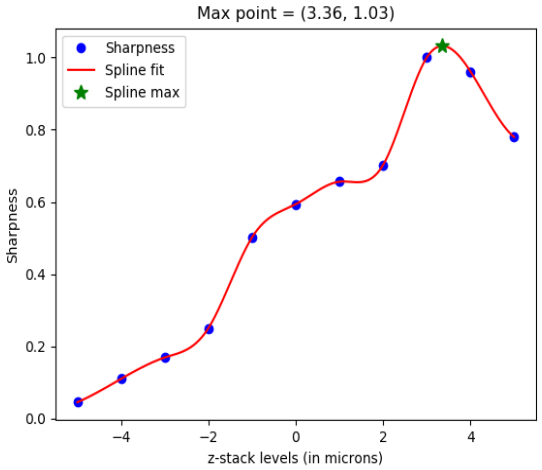

Figure 4: A cubic spline was interpolated through values of sharpness measure across z-layers. Instead of choosing the z-coordinate of a neuron from one of the z-levels, a continuous value where the spline achieves maximal value is chosen instead (green star).

III. Results

In this section we show results from processing a stack of 11 images, produced by scanning a chosen area of a histological section at z-levels in range from -5µm to +5µm, with a step of 1µm, at magnification of 40x. Images captured were of size 4096x4096 pixels corresponding to tissue area of approximately 0.86mm^2. Our neuronal localization algorithm was implemented using Python programming language. The time needed to process the whole stack and obtain 3D locations of neurons was under a minute using an average personal computer with Intel i5-4300U processor with 12Gb of memory. Most of the computation time was spent for performing the watershed algorithm and determining areas of neuron bodies.

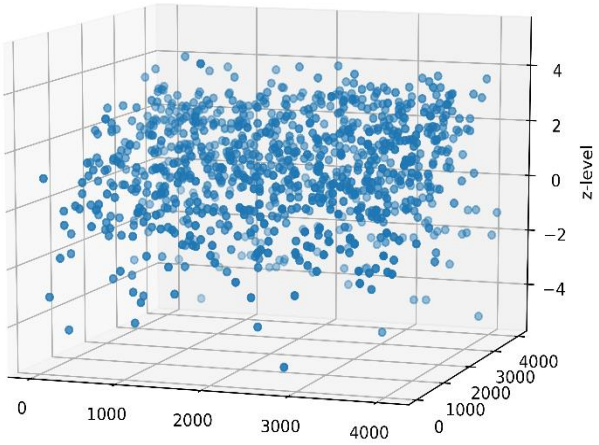

Figure 5: Visualization of 3D locations of all neurons found in the image stack. Values of z-coordinates are continuous instead of limited to the z-level offset due to the spline interpolation of measured sharpness values for each neuron.

IV. Conclusion

In this paper we presented a method for inferring a third spatial dimension for a given 2D neuron locations in a bright-field image of a histological slide of human brain scanned at multiple z-layers. A watershed algorithm was used to segment neuron bodies, which we tracked across all the images in the stack and measured the level of sharpness at each z-level. Variance of Laplacian was used as a sharpness measure, as a common measure in microscopy. Finally, to produce a more realistic values of z-coordinates, we interpolated a cubic spline through measured sharpness values for each neuron and instead of choosing a value from the z-level offsets, for the third spatial coordinate we chose the value for which the interpolated spline achieved a maximum.

Acknowledgment

This publication was co-financed by the Canada First Research Excellence Fund, awarded to McGill University for the Healthy Brains for Healthy Lives initiative and the European Union through the European Regional Development Fund, Operational Programme Competitiveness and Cohesion, grant agreement No. KK.01.1.1.01.0007, CoRE - Neuro.

References

[1] Farahani, N., Parwani, A. V., & Pantanowitz, L. (2015). Whole slide imaging in pathology: advantages, limitations, and emerging perspectives. Pathol Lab Med Int, 7, 23-33.

[2] Parekh, R., & Ascoli, G. A. (2013). Neuronal morphology goes digital: a research hub for cellular and system neuroscience. *Neuron*, 77(6), 1017-1038.

[3] Wilson, M. (2017). Introduction to Widefield Microscopy, *Leica Microsystems*

[4] Ross, J. D., Cullen, D. K., Harris, J. P., LaPlaca, M. C., & DeWeerth, S. P. (2015). A three-dimensional image processing program for accurate, rapid, and semi-automated segmentation of neuronal somata with dense neurite outgrowth. Frontiers in neuroanatomy, 9, 87.

[5] Mathew, B., Schmitz, A., Muñoz-Descalzo, S., Ansari, N., Pampaloni, F., Stelzer, E. H., & Fischer, S. C. (2015). Robust and automated three-dimensional segmentation of densely packed cell nuclei in different biological specimens with Lines-of-Sight decomposition. *BMC bioinformatics*, *16*(1), 187.

[6] Oberlaender, M., Dercksen, V. J., Egger, R., Gensel, M., Sakmann, B., & Hege, H. C. (2009). Automated three-dimensional detection and counting of neuron somata. Journal of neuroscience methods, 180(1), 147-160.

[7] Lafarge, M. W., Pluim, J. P., Eppenhof, K. A., Moeskops, P., & Veta, M. (2018). Inferring a Third Spatial Dimension from 2D Histological Images. *arXiv preprint arXiv:1801.03431*.

[8] Amunts, K., Lepage, C., Borgeat, L., Mohlberg, H., Dickscheid, T., Rousseau, M. É., Shah, N. J. et al. (2013). BigBrain: an ultrahigh-resolution 3D human brain model. *Science*, *340*(6139), 1472-1475.

[9] Judaš, M., Šimić, G., Petanjek, Z., Jovanov-Milošević, N., Pletikos, M., Vasung, L., & Kostović, I. (2011). The Zagreb Collection of human brains: a unique, versatile, but underexploited resource for the neuroscience community. *Annals of the New York Academy of Sciences*, *1225*(1).

[10] Deroulers, C., Ameisen, D., Badoual, M., Gerin, C., Granier, A., & Lartaud, M. (2013). Analyzing huge pathology images with open source software. *Diagnostic pathology*, *8*(1), 92.

[11] Štajduhar, A., Džaja, D., Judaš, M., Lončarić, S. (2018). Automatic Detection of Neurons in NeuN-stained Histological Images of Human Brain. *arXiv preprint arXiv 1806.00292*

[12] Otsu, N. (1979). A threshold selection method from gray-level histograms. *IEEE transactions on systems, man, and cybernetics*, *9*(1), 62-66.

[13] Pertuz, S., Puig, D., & Garcia, M. A. (2013). Analysis of focus measure operators for shape-from-focus. *Pattern Recognition*, *46*(5), 1415-1432.

[14] Pech-Pacheco, J. L., Cristóbal, G., Chamorro-Martinez, J., & Fernández-Valdivia, J. (2000). Diatom autofocusing in brightfield microscopy: a comparative study. In *Pattern Recognition, 2000. Proceedings. 15th International Conference on* (Vol. 3, pp. 314-317). IEEE.